Constraints on the onset of color transparency from quasi-elastic ^{12}C(e,e'p).

D. Bhetuwal,[1] J. Matter,[2] H. Szumila-Vance,[3] L. Kabir,[1] D. Dutta,[1] R. Ent,[3] D. Abrams,[2] Z. Ahmed,[4] B. Aljawrneh,[5] S. Alsalmi,[6] R. Ambrose,[4] D. Androic,[7] W. Armstrong,[8] A. Asaturyan,[9] K. Assumin-Gyimah,[1] C. Ayerbe Gayoso,[10,1] A. Bandari,[10] S. Basnet,[4] V. Berdnikov,[11] H. Bhatt,[1] D. Biswas,[12] W. Boeglin,[13] P. Bosted,[10] E. Brash,[14] M. Bukhari,[15] H. Chen,[2] J.P. Chen,[3] M. Chen,[2] E.M. Christy,[12] S. Covrig,[3] K. Craycraft,[16] S. Danagoulian,[5] D. Day,[2] M. Diefenthaler,[3] M. Dlamini,[17] J. Dunne,[1] B. Duran,[8] R. Evans,[4] H. Fenker,[3] N. Fomin,[16] E. Fuchey,[18] D. Gaskell,[3] T. N. Gautam,[12] F. A. Gonzalez,[19] O. Hansen,[3] F. Hauenstein,[20] A. V. Hernandez,[11] T. Horn,[11] G. Huber,[4] M. K. Jones,[3] S. Joosten,[8] A. Karki,[1] C. Keppel,[3] A. Khanal,[13] P. King,[17] E. Kinney,[21] H. S. Ko,[22] M. Kohl,[12] N. Lashley-Colthirst,[12] S. Li,[23] W. Li,[10] A. H. Liyanage,[12] D. Mack,[3] S. Malace,[3] P. Markowitz,[13] D. Meekins,[3] R. Michaels,[3] H. Mkrtchyan,[9] S.J. Nazeer,[12] S. Nanda,[1] G. Niculescu,[24] M. Niculescu,[24] D. Nguyen,[2] Nuruzzaman,[25] B. Pandey,[12] S. Park,[19] E. Pooser,[3] A. Puckett,[18] M. Rehfuss,[8] J. Reinhold,[13] N. Santiesteban,[23] B. Sawatzky,[3] G. Smith,[3] A. Sun,[26] V. Tadevosyan,[9] R. Trotta,[11] S. A. Wood,[3] C. Yero,[13] and J. Zhang[19]

(for the Hall C Collaboration)

[1]*Mississippi State University, Mississippi State, Mississippi 39762, USA*
[2]*University of Virginia, Charlottesville, Virginia 22903, USA*
[3]*Thomas Jefferson National Accelerator Facility, Newport News, Virginia 23606, USA*
[4]*University of Regina, Regina, Saskatchewan S4S 0A2, Canada*
[5]*North Carolina A & T State University, Greensboro, North Carolina 27411, USA*
[6]*Kent State University, Kent, Ohio 44240, USA*
[7]*University of Zagreb, Zagreb, Croatia*
[8]*Temple University, Philadelphia, Pennsylvania 19122, USA*
[9]*Yerevan Physics Institute, 375036 Yerevan, Armenia*
[10]*The College of William & Mary, Williamsburg, Virginia 23185, USA*
[11]*Catholic University of America, Washington, DC 20064, USA*
[12]*Hampton University, Hampton, Virginia 23669, USA*
[13]*Florida International University, University Park, Florida 33199, USA*
[14]*Christopher Newport University, Newport News, Virginia 23606, USA*
[15]*Jazan University, Jazan 45142, Saudi Arabia*
[16]*University of Tennessee, Knoxville, Tennessee 37996, USA*
[17]*Ohio University, Athens, Ohio 45701, USA*
[18]*University of Connecticut, Storrs, Connecticut 06269, USA*
[19]*Stony Brook University, Stony Brook, New York 11794, USA*
[20]*Old Dominion University, Norfolk, Virginia 23529, USA*
[21]*University of Colorado Boulder, Boulder, Colorado 80309, USA*
[22]*Institut de Physique Nucleaire, Orsay, France*
[23]*University of New Hampshire, Durham, New Hampshire 03824, USA*
[24]*James Madison University, Harrisonburg, Virginia 22807, USA*
[25]*Rutgers University, New Brunswick, New Jersey 08854, USA*
[26]*Carnegie Mellon University, Pittsburgh, Pennsylvania 15213, USA*

(Dated: September 28, 2020)

Quasielastic ^{12}C$(e, e'p)$ scattering was measured at momentum transfer squared $Q^2 = 8$, 9.4, 11.4, and 14.2 (GeV/c)^2, the highest ever achieved to date. Nuclear transparency for this reaction was extracted by comparing the measured yield to that expected from a plane-wave impulse approximation calculation without any final state interactions. The measured transparency was observed to be independent of Q^2, up to momentum scales where earlier $A(p, 2p)$ results had indicated a rise in transparency, ruling out the quantum chromodynamics effect of color transparency at such momentum scales. These results impose strict constraints on models of color transparency for protons.

One of the dominant elements of the nuclear many body problem governing the propagation of hadrons through the nuclear medium is a "reduction of flux". For example, in the quasielastic scattering of electrons from a nucleus, $A(e, e'p)$, the outgoing proton in the elementary ep elastic scattering can undergo final state interactions (FSI) with the spectator nucleons. These interactions can lead to the absorption and/or rescattering of the outgoing proton resulting in the reduction of the measured $A(e, e'p)$ yield, where the scattered electron and proton are detected in coincidence. This reduction of the coincidence yield can be quantified in terms of the nuclear transparency (T), defined for the $A(e, e'p)$ process as the ratio of the measured to the calculated Plane Wave Impulse Approximation (PWIA) yield. The PWIA yield is calculated in the absence of FSI as well as initial state interactions (ISI). Nuclear transparency for the $A(e, e'p)$ process is then the probability that the knocked-out proton escapes the nucleus without further interactions with the spectator nucleons. Thus, the measurement of T remains of active interest for insight into the nuclear many body problem and the strong interaction between hadrons and nuclei [1]

At low energies, the strong interaction is well described in terms of nucleons (protons and neutrons) exchanging mesons, whereas at high energies, perturbative Quantum Chromodynamics (pQCD) characterizes the strong force in terms of quarks and gluons carrying color charge. Although these two descriptions are well understood in their respective energy scales, the transition between them is not uniquely identified. Quantum Chromodynamics (QCD) predicts that protons produced in exclusive processes at sufficiently high momentum transfers (Q), will experience suppressed final (initial) state interactions resulting in a significant enhancement in the nuclear transparency [2]. This unique prediction of QCD is named color transparency (CT), and the observation of the onset of CT may help identify the transition between the two alternate descriptions of the strong force. Measurement of T can therefore test for deviation from the expectations of conventional nuclear physics and the onset of quark-gluon degrees of freedom.

Mueller and Brodsky [2] introduced CT as a direct consequence of the concept that in exclusive processes at sufficiently high momentum transfer, hadrons are produced in a small point-like configuration (PLC). Quantum mechanics accounts for the existence of hadrons that fluctuate to a PLC, and a high momentum transfer virtual photon preferentially interacts with a hadron in a PLC (with transverse size $r_\perp \approx 1/Q$). This phenomenon is sometimes referred to as "squeezing" [3]. The reduced transverse size, color neutral PLC is screened from external fields, analogous to a reduced transverse size electric dipole [3]. At high energies, due to relativistic time dilation (referred to as "freezing"), the PLC maintains its compact size long enough to traverse the nuclear volume experiencing reduced interaction with the spectator nucleons. It thereby experiences reduced attenuation in the nucleus due to color screening and the properties of the strong force [3]. The onset of CT is thus a signature of QCD degrees of freedom in nuclei and is expected to manifest as an increase in T with increasing momentum transfer.

CT is well-established at high energies, see for example Ref. [1], but the energy regime for the onset of CT is less well known. In fact, the suppression of further interactions with the nuclear medium is a fundamental assumption necessary to account for Bjorken scaling in deep-inelastic scattering at small x_B [4]. Moreover, the onset of CT is of specific interest as it can help identify the relevant momentum transferred squared (Q^2) where factorization theorems are applicable [5] enabling the extraction of Generalized Parton Distributions (GPDs) [6, 7]. At intermediate energies, there exists a trade off between the selection of the PLC and its expansion as it transits the nucleus. Therefore the onset of CT is best observed at the intermediate energy regime where the expansion distance of the PLC becomes significant compared to the nuclear radius. Theory anticipates that it is more probable to observe the onset of CT at lower energies for meson production than for baryons as it is more probable to for quark-anti-quark pairs (mesons) to form a PLC than three quark systems (baryons) [8]. Additionally, the expansion distance over which the PLC fluctuates back to its equilibrium configuration, is larger than the nuclear radius at lower energies for mesons than for baryons [9].

The predicted onset of CT for final-state mesons has been demonstrated in several experiments at Jefferson Lab (JLab). Pion photoproduction cross section of ^{4}He to ^{2}H demonstrated deviations from Glauber that was consistent with CT theories showing a positive rise in the cross section ratio [10]. Precise and systematic studies of pion electroproduction on a range of targets established a positive slope in the transparency ratios for Q^2 in the range from 1–5 (GeV/c)^2, as well as an A-dependence of the slope. These results were found to be consistent with models that include CT [11, 12]. The onset of CT is mesons was further confirmed by a JLab experiment measuring the nuclear transparency of ρ^0 electroproduction which showed slopes vs Q^2 consistent with the same CT models [13] as the pions. While empirical evidence conclusively confirms the onset of CT in mesons at momentum scales corresponding to $Q^2 \sim 5$ (GeV/c)^2, the observation of the onset of CT in baryons is somewhat ambiguous.

In a pioneering experiment at the Brookhaven National Lab (BNL), the E850 collaboration attempted to measure the onset of CT using a large angle proton knockout $A(p, 2p)$ reaction [14]. The nuclear transparency was measured as the ratio of the quasielastic cross section from a nuclear target to that of the free pp cross section. The transparency was measured as a function of an effective beam momentum, P_{eff}, and was shown to have a positive rise, consistent with CT, from $P_{\text{eff}} = 5.9$–9 GeV/c [14]. However, a subsequent decrease in the transparency was observed between $P_{\text{eff}} =$ 9.5–14.4 GeV/c that was not consistent with CT [15–17]. This enhancement and subsequent fall in the nuclear transparency spans a Q^2 (Mandelstam $-t$) range of 4.8–12.7 (GeV/c)^2 and outgoing proton momentum range of 3.3–7.7 GeV/c. Two possible explanations for the decrease in transparency at the higher momenta are; an in-medium suppression of the energy dependence of the pp elastic cross section known as nuclear filtering [18] [19], or the excitation of charmed quark resonances or other exotic multi-quark states [20].

In the $A(p,2p)$ reaction both the incoming and outgoing protons experience a reduction of flux making it more challenging to interpret. Consequently, the ambiguous results from the BNL experiment were investigated with the $(e,e'p)$ process, which employs electrons, a weakly interacting probe, to avoid the complication of the reduction of flux of the hadronic probe. Further, compared to the $(p,2p)$ process, the elementary ep scattering cross section is accurately known and smoothly varying, and the $A(e,e'p)$ process is less sensitive to the poorly known large momentum components of the nuclear wave function [21].

Previous $A(e,e'p)$ experiments [22–25] have measured the nuclear transparency of protons on a variety of nuclei up to $Q^2 = 8.1$ (GeV/c)^2. These experiments yielded missing energy and momentum distributions consistent with conventional nuclear physics and did not observe any Q^2 dependence in the nuclear transparency. This ruled out the onset of CT for protons at Q^2 values corresponding to outgoing proton momenta of 5 GeV/c, which in some interpretations is just before the rise of transparency noted in the $A(p,2p)$ data.

The recent 12 GeV upgrade at Jefferson Lab allows access to the entire Q^2 range and outgoing proton momentum range of the BNL experiment for the first time. It also allows significant overlap between the knocked out proton momentum in electron scattering and the effective proton momentum quoted by the BNL experiment $A(p,2p)$ experiment, within the range where the enhancement in nuclear transparency was observed [14]. These features make it possible to explore all possible variables (Q^2, incident or outgoing proton momentum) that could be driving the said enhancement in transparency observed in the BNL experiment. In this letter we report on the latest quasi-elastic electron scattering experiment to search for the onset of CT at the upgraded JLab. This experiment extends the nuclear transparency measurements in $^{12}C(e,e'p)$ to the highest Q^2 to date and exhaustively covers the complete kinematic phase space of the enhancement observed by the BNL experiment.

The experiment was carried out in Hall C at JLab and was the first experiment to be completed in Hall C after the upgrade of the continuous wave (cw) electron beam facility (CEBAF) accelerator. The experiment used the cw electron beam from the CEBAF accelerator with beam energies of 6.4 and 10.6 GeV and beam currents up to 65 μA. The total accumulated beam charge was determined with $< 1\%$ uncertainty by a set of resonant cavity based beam current monitors and a parametric transformer monitor. The beam energy was determined with an uncertainty of 0.1% by measuring the bend angle of the beam, on its way into Hall-C, as it traversed a set of magnets with precisely known field integrals. The main production target was a carbon foils of 4.9% radiation lengths (rl), and a second carbon foil of 1.5% rl was used for systematic studies. The thickness of the foils were determined to better than 0.5%. A 10 cm long (726 mg/cm^2) liquid hydrogen target was used for normalization to the elementary ep scattering process, and a 10 cm aluminum empty target was used to monitor the background from the aluminum end caps of the hydrogen target cell. The beam incident on the liquid hydrogen target was rastered over a 2×2 mm^2 area to suppress density variations from localized boiling.

The scattered electrons were detected in the existing High Momentum Spectrometer (HMS, momentum acceptance $\Delta p/p \pm 10\%$, solid angle $\Omega = 7$ msr) [24] in coincidence with the knocked out protons detected in the new Super High Momentum Spectrometer (SHMS, momentum acceptance $\Delta p/p$ from -10 to +12%, solid angle $\Omega = 4$ msr) [26]. The SHMS central angle was chosen to detect protons along the three momentum transfer, $\vec{q}$. The kinematics of the four different Q^2 settings are shown in Table I. The solid angle of the spectrometers was defined for electrons and the coincident $(e,e^{'}p)$ process by a 2-in. thick heavymet (a tungsten alloy) collimator. The detector packages in the two spectrometers were similar, they included four planes of segmented scintillators (except for the last plane in SHMS which used quartz bars) that were used to form the trigger and to provide time of flight information. Two 6-plane drift chambers were used to measure particle tracks with better than 250-μm resolution. The tracking efficiency was continuously monitored with an uncertainty of ∼0.1% for the HMS and < 0.5% for the SHMS. The uncertainty was obtained from the average variation of the tracking efficiency when using three independent criteria for determining the efficiency. The typical momentum and angular resolution in the HMS (SHMS) were 0.2% (0.1%) for momentum, 0.8 (0.9) mr for horizontal angle and 1.2 (1.1) mr for the vertical angle. In the HMS a threshold gas Čerenkov detector and a segmented Pb-glass calorimeter were used for electron identification. The protons in the SHMS were identified using a noble gas threshold Čerenkov detector and a segmented Pb-glass calorimeter to reject pions. The pion-to-electron ratio in the HMS ranged from $\sim 10^{-1}$ to 10^{-3}, while the pion-to-proton ratio in the SHMS was always < 0.2. The corrections

TABLE I. Kinematics

$\mathbf{Q^2}$ $((\mathbf{GeV/c})^2)$	$\theta_{\mathbf{e'}}^{lab}$ (deg)	$p_{\mathbf{e'}}$ (GeV/c)	$\theta_{\mathbf{p}}^{lab}$ (deg)	$p_{\mathbf{p}}$ (GeV/c)
8.0	45.1	2.125	17.1	5.030
9.4	23.2	5.481	21.6	5.830
11.4	28.5	4.451	17.8	6.882
14.2	39.3	2.970	12.8	8.352

for particle energy loss through the spectrometers were determined to better than 1%. The electron-proton coincidence events were recorded in 1-hour long runs via a pipelined data acquisition system operated using the CEBAF Online Data Acquisition (CODA) software package [27]. Singles (inclusive) electron and proton events were separately recorded for systematic studies.

The individual electron and proton tracks for each coincidence event were reconstructed back to the target. The coincidence time was determined as the difference in the time of flight between the two spectrometers with corrections to account for path length variations from the central trajectory and the individual start times. The coincidence time spectrum had a width of 380 ps, sufficiently smaller than the 4-ns beam structure. The rate of accidental coincidences was $< 0.2\%$.

At each kinematic setting, the charge normalized experimental yield for ep coincidences measured on the hydrogen target, was compared to a parameterization of the known ep elastic scattering cross section [28] through a Monte Carlo simulation of the experiment [29] (see Fig. 1). The simulation included a realistic model of the spectrometer magnetic transport properties, the detailed geometries of all the detectors and intervening materials, and models for processes such as multiple scattering, ionization energy loss and radiative effects. The experimental yield was corrected for detector and tracking inefficiencies, computer and electronic dead-times and proton absorption in SHMS. The density of the liquid hydrogen target varies with the incident electron beam current (beam boiling effect), and the experimental yield was corrected for this effect. The correction was determined to be $(2.3\pm0.4)\%$ at the highest beam current (65 μA). The hydrogen yield was found to be consistent with the known ep elastic scattering world data, validating the analysis procedure. The comparison to the Monte Carlo yield was used to determine the normalization uncertainty of $\pm$ 1.8%.

The electron beam energy/momentum $(E_e/\vec{p}_e)$ and the energy/momentum of the scattered electron $(E_{e'}/\vec{p}_{e'})$ measured by the HMS was used to determine $\vec{q} = \vec{p}_e - \vec{p}_{e'}$ and the energy transfer $\nu = E_e - E_{e'}$ for each coincidence event. The kinetic energy $(T_{p'})$ and momentum $(\vec{p}_{p'})$ of knocked out protons measured in the SHMS was used to determine the missing energy $E_m = \nu - T_{p'} - T_{A-1}$ and missing momentum $\vec{p}_m = \vec{p}_{p'} - \vec{q}$ for the coincidence event, where T_{A-1} is the reconstructed kinetic energy of the $A-1$ recoiling nucleus. The experimental yield on the ^{12}C target was obtained by integrating the charge normalized coincidence events over a phase space defined by E_m <80 MeV and $|\vec{p}_m|$ <300 MeV/c. These constraints eliminate inelastic contributions such as from pion production and ensure exclusivity. The experimental yield was corrected for all known inefficiencies of both spectrometers such as the detector efficiencies (97% - 99%), trigger efficiency (98% - 99%), tracking efficiencies (99%-HMS and 94% - 99%-SHMS), computer and electronic livetimes (94% - 99%), and proton absorption in the SHMS ($\sim$ 8%). The systematic uncertainty of the experimental yield arising from the event selection constraints for particle identification and on the spectrometer acceptance was determined by varying the constraints one at a time and recording the variation in yields over the different kinematic settings. The quadrature sum over all of the different types of constraints was used as the event selection uncertainty ($\sim$1.4%). The uncertainty due to the livetime and the detector and trigger efficiencies was determined from a set of luminosity scans in each spectrometer performed immediately before and after the experiment on a ^{12}C target. The charge normalized yield from these scans for each spectrometer was found to be independent of the beam current within statistical uncertainties, and the average variation in the normalized yield vs beam current was recorded as the systematic uncertainty (0.5%). The variation in the charge normalized experimental yield was <1% when using using all events with beam current above 5 μA or a more restrictive cut of $\pm$ 3 μA around the average current (for each interval with stable current). This validates the $< 1\%$ uncertainty estimated for the charge measurement.

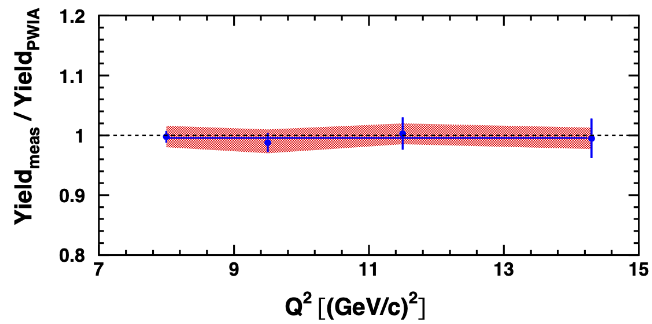

FIG. 1. The ratio of measured yield to the simulation (SIMC) yield is shown for elastic ep scattering from hydrogen for E_m < 65 MeV and $|p_m|$ < 65 MeV/c. Only the statistical uncertainty are shown. The solid horizontal line is a fit to a constant value with the shaded band representing the the normalization uncertainty of 1.8% determined from these yield ratios and includes the $\sim$1% variation in the ratio when the E_m and $|p_m|$ cuts are varied.

A Monte Carlo simulation of the $A(e, e'p)$ process was performed assuming the plane-wave impulse approximation (PWIA) to be valid, in which case the $\vec{p}_m$ is equal to the initial momentum of the proton in the carbon nucleus, and the cross section is calculated in a factorized form as:

$$\frac{d^6\sigma}{dE_{e'}d\Omega_{e'}dE_{p'}d\Omega_{p'}} = E_{p'}|p_{p'}|\sigma_{ep}S(E_m, \vec{p}_m), \qquad (1)$$

where $\Omega_{e'}$, $\Omega_{p'}$ are the solid angles of the outgoing electron and proton respectively, σ_{ep} is the off-shell ep cross section and $S(E_m, \vec{p}_m)$ is the spectral function defined as the joint probability of finding a proton with momentum p_m and separation energy E_m within the nucleus. The simulation used the De Forest σ_1^{cc} prescription [30] for the off-shell cross section, and the simulated yield was insensitive ($< 0.1\%$) to the off-shell effect. The independent particle spectral functions used in the simulation were same as the ones used Ref. [22–25]. The effect of nucleon-nucleon correlations, which causes the single particle strength to appear at high E_m, was included by applying a correction factor of 1.11 ± 0.03 as previously determined in Ref. [31]. The simulated yield was obtained by integrating over the same phase space volume as for the experimental data. The total model dependent uncertainty due to the uncertainty in the model spectral function (2.8%) and the corrections due to nucleon-nucleon correlations, was estimated to be 3.9%.

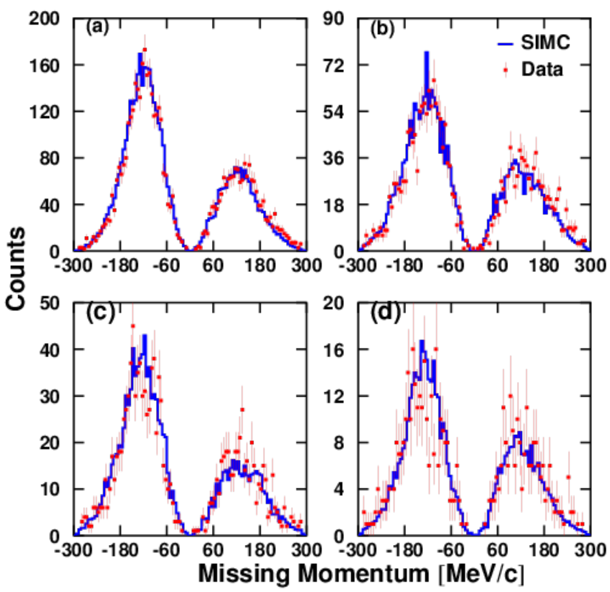

FIG. 2. The missing momentum, p_m, for the Carbon data is shown for each kinematic setting. (a) $Q^2 = 8.0$ (b) $Q^2 = 9.4$ (c) $Q^2 = 11.4$ and (d) $Q^2 = 14.2\,(\mathrm{GeV/c})^2$

The $^{12}\mathrm{C}(e, e'p)$ yields as a function of P_m are shown in Fig 2, along with the simulated yields. The constraint of $E_m < 80$ MeV was applied to both data and simulation. The shape of the data and simulated distributions agree with each other very well for all four Q^2 settings validating the use of the impulse approximation. It also indicated the robustness of the spectrometer models in the Monte Carlo simulation. The uncertainty from the spectrometer acceptance was estimated to be 2.6% by comparing the measured and simulated focal plane positions and angles as well as the reconstructed angles and momenta at the reaction vertex. The p_m distributions shown in Fig. 2, are very sensitive to the reconstructed momenta and angles, and the average bin-by-bin difference between the data and simulated spectra normalized to each other was used as the systematic uncertainty due to acceptance. Table II lists the major sources of systematic uncertainty. The total uncertainty is calculated as the quadrature sum. The model dependent uncertainty is not included in the table.

TABLE II. Systematic Uncertainties

Source	Q^2 dependent uncertainty (%)
Spectrometer acceptance	2.6
Event selection	1.4
Tracking efficiency	0.5
Radiative corrections	1.0
Live time & Det. efficiency	0.5
Source	Normalization uncertainty (%)
Free cross section	1.8
Target thickness	0.5
Beam charge	1.0
Proton absorption	0.5
Total	3.9

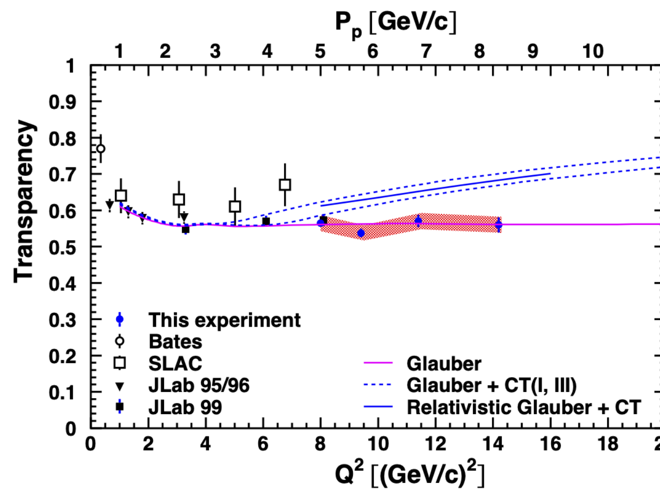

FIG. 3. The carbon nuclear transparency from this experiment along with all previous experiments [22–25, 32]. The 4-momentum transfer squared is shown along the $x-$axis (bottom scale), and the momentum of the knocked out proton is also shown along the top scale of the $x-$axis. The solid magenta line is a Glauber calculation that excludes color transparency effects [33]. The dashed lines are theory predictions including CT [34] for two different set of parameters and the solid blue line is a prediction from a relativistic Glauber calculation with CT [35]. The error bars show the statistical uncertainty while the band shows the systematic uncertainty. The additional model dependent uncertainty is not shown.

The nuclear transparency was extracted as the ratio of experimental yield to the PWIA yield integrated over the same phase space volume V:

$$T(Q^2) = \frac{\int_V d^3p_m dE_m Y_{exp}(E_m, \vec{p}_m)}{\int_V d^3p_m dE_m Y_{\mathrm{PWIA}}(E_m, \vec{p}_m)}, \qquad (2)$$

where V is the phase space volume as defined earlier, $Y_{exp}(E_m, \vec{p}_m)$ is the experimental yield and $Y_{\rm PWIA}(E_m, \vec{p}_m)$ is the PWIA yield. The extracted nuclear transparency as a function of Q^2 is shown in Fig. 3 along with all previous measurements. The measured nuclear transparency of carbon is found to be both energy and Q^2 independent up to $Q^2 = 14.2\,({\rm GeV/c})^2$, the highest accessed in quasi-elastic electron scattering to date. The combined data set from all measurements above $Q^2 = 3.0\,({\rm GeV/c})^2$ was fit to a constant value with a reduced χ^2 of 1.3. The outgoing proton momentum of this experiment overlaps with the effective proton momentum of the BNL experiments that reported an enhancement in nuclear transparency[17]. Moreover, the Q^2 and outgoing proton momentum of this experiment is significantly higher than the BNL experiment. Hence, these results rule out CT as a possible cause of the rise in transparency observed by the BNL experiment. The differences governing the observed onset of CT for mesons at Q^2 (outgoing meson momentum) scales of 1 (GeV/c)^2 (2.5 GeV/c) and the ruled-out onset of CT for protons at Q^2 (outgoing proton momentum) scales of 14 (GeV/c)^2 (8 GeV/c) may provide strong clues regarding the differences between two- and three-quark systems. Future experiments at JLab and elsewhere will further quantify such differences for pions, ρ-mesons and photons [36–38].

In summary, exclusive measurements were performed for Q^2 from 8–14.2 (GeV/c)^2 on hydrogen and carbon targets. The nuclear transparency extracted from these measurements are consistent with traditional nuclear physics calculation and do not support the onset of color transparency. The momentum scales accessed in this experiment rule out color transparency as the reason for a rise in transparency noted in $A(p, 2p)$ data. The present results probe down to a transverse-size as small as $\sim$0.05 fm in the three-quark nucleon system, placing very strict constraints on the onset of color transparency at intermediate energies and all current models.

This work was funded in part by the U.S. Department of Energy, including contract AC05-06OR23177 under which Jefferson Science Associates, LLC operates Thomas Jefferson National Accelerator Facility, and by the U.S. National Science Foundation. We wish to thank the staff of Jefferson Lab for their vital support throughout the experiment. We are also grateful to all granting agencies providing funding support to authors throughout this project.

[1] D. Dutta, K. Hafidi, and M. Strikman. Color transparency: past, present and future. *Progress in Particle and Nuclear Physics*, 69:10, 2012.
[2] A. H. Mueller. Proceedings of the Seventeenth Recontre de Moriond Conference on Elementary Particle Physics. Les Arcs, France, 1983.
[3] S. J. Brodsky, L. Frankfurt, J. F. Gunion, A. H. Mueller, and M. Strikman. *Phys. Rev. D*, 50:3134, 1994.
[4] L. Frankfurt and M. Strikman. *Phys Rep.*, 160:235, 1988.
[5] M. Strikman. *Nucl. Phys. A*, 663-664:64c–73c, 2000.
[6] X. Ji. *Phys. Rev. Lett.*, 78:610, 1997.
[7] A. V. Radyushkin. *Phys. Rev. D*, 56:5524–5557, Nov 1997.
[8] M. Eides, L. Frankfurt, and M. Strikman. *Phys. Rev. D*, 59:114025, 1999.
[9] M. Vanderhaeghen, P. A. M. Guichon, and M. Guidal. *Phys. Rev. D*, 60:094017, 1999.
[10] D. Dutta et al. *Phys. Rev. C*, 68:021001R, 2003.
[11] B. Clasie et al. *Phys. Rev. Lett.*, 99:242502, 2007.
[12] X. Qian et al. *Phys Rev. C*, 81:055209, 2010.
[13] L. El-Fassi et al. *Phys. Lett. B*, 712:326, 2012.
[14] A. S. Carroll et al. *Phys. Rev. Lett.*, 61:1698, 1988.
[15] I. Mardor et al. *Phys. Rev. Lett.*, 81:5085, 1998.
[16] A. Leksanov et al. *Phys. Rev. Lett.*, 87:212301, 2001.
[17] J. Aclander et al. *Phys. Rev. C*, 70:015208, Jul 2004.
[18] J. P. Ralston and B. Pire. *Phys. Rev. Lett.*, 61:1823, 1990.
[19] B. Kundu, J. Samuelsson, P. Jain, and J. P. Ralston. *Phys. Rev. D*, 62:113009, 2000.
[20] S. J. Brodsky and G. F. de Teramond. *Phys Rev. Lett.*, 60:1924, 1988.
[21] G. R. Farrar, H. Liu, L. L. Frankfurt, and M. I. Strikman. *Phys. Rev. Lett.*, 62:1095, 1989.
[22] N. C. R. Makins et al. *Phys. Rev. Lett*, 72:1986, 1994.
[23] T. G. O'Neill et al. *Phys. Lett.*, 351:87, 1995.
[24] D. Abbott et al. *Phys. Rev. Lett.*, 80:5072, 1998.
[25] K. Garrow et al. *Phys. Rev. C*, 66:044613, 2002.
[26] The SHMS spectrometer in Hall-C. *publication in preparation.*
[27] `https://coda.jlab.org/drupal/`.
[28] P. Bosted. *Phys. Rev. C*, 51:409, 1995.
[29] `https://hallcweb.jlab.org/simc/`.
[30] T. De Forest. *Nucl. Phys. A*, 392(2):232 – 248, 1983.
[31] T. G. O'Neill. PhD thesis, California Institute of Technology (unpublished), 1994.
[32] G. Garino et al. *Phys. Rev. C*, 45:780, 1992.
[33] V. R. Pandharipande and S. C. Pieper. *Phys. Rev. C*, 45:791, 1992.
[34] L. L. Frankfurt et al. *Phys. Rev. C*, 51:3435, 1995.
[35] W. Cosyn, M. C. Martinez, J. Ryckebusch, and B. Van Overmeire. *Phys. Rev. C*, 74:062201(R), 2006.
[36] D. Dutta, R. Ent, K. Garrow, et al. Proposal for JLab experiment E01-107.
[37] K. Hafidi, B. Mustapa, M. Holtrop, et al. Proposal for JLab experiment E12-07-103.
[38] A. Somov, O. Hen, et al. Proposal for JLab experiment PR12-17-007.